Heparanase and Vascular Endothelial Growth Factor Expression Is Increased in Hypoxia-Induced Retinal Neovascularization

Jie Hu,[1] *Xin Song,*[1] *Yi Qing He,*[2,3] *Craig Freeman,*[3] *Christopher R. Parish,*[3] *Ling Yuan,*[1] *Honghua Yu,*[1] *and Shibo Tang*[1]

Purpose. Heparanase and VEGF are related closely to angiogenesis in cancer. The purpose of our study was to evaluate the expression and correlation of heparanase and VEGF in hypoxia-induced retinal neovascularization.

Methods. C57BL/6 oxygen-induced retinopathy (OIR) mice and human retinal microvascular endothelial cells (HRECs) were treated with the hypoxia mimetic agent cobalt chloride ($CoCl_2$), and in the presence of the heparanase inhibitor phosphomannopentaose sulfate (Muparfostat, PI-88). Heparanase activity was assayed in HRECs, and the expression of heparanase, VEGF protein and mRNA were evaluated by immunofluorescence, ELISA, Western blot, and real-time PCR while retinal flat mounts were used to evaluate the area of neovascularization of mice retina.

Results. HREC heparanase activity was increased by treatment with $CoCl_2$, but was decreased by PI-88. Immunofluorescence showed that heparanase and VEGF staining was intense in hypoxia-treated HRECs and OIR mice retina, while VEGF staining was faint in the normoxia and PI-88–treated ones. Western blot and real-time PCR results indicated that the expression of heparanase and VEGF was increased under hypoxic conditions, and the increase of VEGF was inhibited by PI-88. Retinal flat mounts showed that the area of new vessels in retina of OIR mice was increased compared to the normoxic mice, and this effect was inhibited by PI-88.

Conclusions. Heparanase is upregulated and associated with the VEGF expression in hypoxia-induced retinal diseases. Heparanase is involved in hypoxia-induced neovascularization through promoting VEGF expression and may be a new therapeutic target for hypoxia-induced neovascularization retinal diseases. (*Invest Ophthalmol Vis Sci.* 2012;53:6810–6817) DOI:10.1167/iovs.11-9144

From the [1]State Key Laboratory of Ophthalmology, Zhongshan Ophthalmic Center, Sun Yat-sen University, Guangzhou, China; the [2]Department of Oral and Maxillofacial Surgery, Guanghua School of Stomatology, Sun Yat-sen University, Guangzhou, China; and the [3]Department of Immunology, The John Curtin School of Medical Research, The Australian National University, Canberra, Australia.

Supported by the International Cooperation Project of Guangdong Province (Grant 2008B050100038), the Fundamental Research Funds of State Key Lab of Ophthalmology, Sun Yat-sen University (Grant 2010C04), and Science and Technology Planning Project of Guangdong Province (Grant 2011B020800005).

Submitted for publication November 23, 2011; revised April 15 and August 12, 2012; accepted August 22, 2012.

Disclosure: **J. Hu**, None; **X. Song**, None; **Y.Q. He**, None; **C. Freeman**, None; **C.R. Parish**, None; **L. Yuan**, None; **H. Yu**, None; **S. Tang**, None

Corresponding author: Jie Hu, The State Key Laboratory of Ophthalmology, Zhongshan Ophthalmic Center, Sun Yat-sen University, Guangzhou 510060, China; hehujie@126.com

Retinopathy of prematurity (ROP) is a leading cause of childhood blindness over the world, characterized by retinal hypoxia-ischemia and neovascularization.[1,2] VEGF, which can be upregulated by hypoxia and ischemia,[3,4] is one of the most significant factors involved in retinal diseases associated with pathologic angiogenesis, including ROP.[5,6] Logically, anti-VEGF therapy has been used in ROP patients and shown beneficial short-term effects.[7,8] However, it has been shown that direct inhibition of VEGF cannot completely prevent the formation of new vessels and anti-VEGF therapy requires long-term, repeated administration to decrease the continuous generated VEGF.[9] Therefore, it is necessary to find a way to inhibit the VEGF protein production for better control of neovascularization.

A very important step in the process of neovascularization is to change the integrity of the extracellular matrix (ECM) and subendothelial basement membrane (BM). Heparanase is an endo-β-glucuronidase that specifically cleaves heparan sulfate (HS) side chains of HS proteoglycans (HSPGs), which are essential components of the cell surface and ECM that provide structural integrity.[10] Thus, heparanase is involved directly in angiogenesis by degrading HS chains. Degradation of HS side chains also releases HS-bound angiogenic growth factors, including FGF-2 and VEGF, and HS fragments, which promote angiogenic growth factor activity.[11]

It is known that cells are exposed to hypoxic environment in solid tumors.[12] Heparanase activity is upregulated by hypoxia in many tumor cells and overexpression of heparanase correlates with increased VEGF protein and mRNA levels, and increased tumor vascularity.[13–15] These studies suggested a correlation between heparanase and hypoxia-induced neovascularization in tumors. Therefore, a similar mechanism was hypothesized in which heparanase regulates VEGF mRNA and protein levels, and promotes neovascularization in ROP. In our study, as an initial step toward understanding the pathophysiologic conditions of ROP, we examined the regulation of heparanase and VEGF expression in retina under normoxic, hypoxic, and hypoxia mimic conditions, and the effect of the heparanase inhibitor, phosphomannopentaose sulfate (Muparfostat, PI-88), on the VEGF expression in vitro and in vivo.

Materials and Methods

Human Retinal Microvascular Endothelial Cell Culture and Treatment

Human eyes were obtained from the Eye Bank of Zhongshan Ophthalmic Center of Sun Yat-sen University (Guangzhou, China), within 20 hours postmortem. Donors of all these eyes were healthy accident victims. All human materials were in compliance with the World Medical Association Declaration of Helsinki ethical principles for

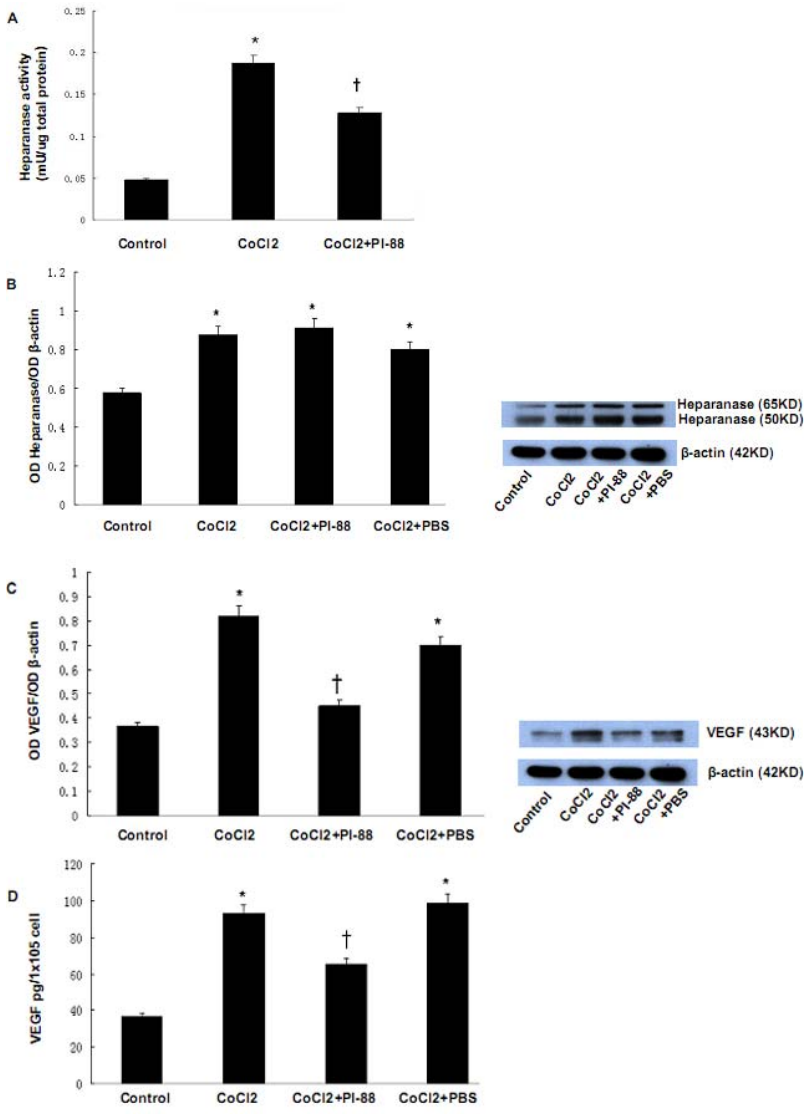

Figure 1. Heparanase activity, heparanase and VEGF protein levels in $CoCl_2$-treated HRECs. HRECs were cultured in normal media (control), or treated with $CoCl_2$, $CoCl_2$ + PI-88, and $CoCl_2$ + PBS for 24 hours. A heparan sulfate degrading enzyme assay kit was used to determine heparanase activity (**A**). Western blot analysis was performed to detect heparanase (**B**) and VEGF (**C**) protein levels. An ELISA was performed on HRECs treated with $CoCl_2$, or $CoCl_2$ + PI-88, and $CoCl_2$ + PBS (**D**). Data represent the mean ± SD of three experiments. $^*P < 0.05$ versus control. †$P < 0.05$ versus $CoCl_2$ or PBS.

medical research. The procedures were as described previously.[16] Briefly, retinal tissues were isolated from eyes, and digested with 2% trypsogen and 0.1% collagenase I (Sigma Chemical Co., St. Louis, MO.) for 20 minutes at 37°C, then subjected to centrifugation (1000*g* for 10 minutes). The pellet was resuspended in human endothelial serum-free medium (Gibco, Grand Island, NY) supplemented with 10% fetal bovine serum (FBS) and 5 ng/mL β-endothelial cell growth factor (β-ECGF, Sigma), plated into a 21.5 mm^2 culture dish precoated with 5 mg/mL fibronectin (Gibco), and then incubated at 37°C with 5% CO_2. Human retinal microvascular endothelial cells (HRECs) were identified by positive staining with anti-VIII factor antibody (Biosynthesis Biotechnology Co., Beijing, China). Only cells at passages 3 to 5 were used for the experiments.

HRECs were incubated with normal medium (normal group), 100 μM cobalt chloride ($CoCl_2$ group), or 100 μM $CoCl_2$ combined with 5 μg/mL heparanase inhibitor PI-88 (PI-88 group; Progen Pharmaceuticals Limited, Brisbane, Australia) for 24 hours.[17] PI-88 was dissolved in sterile PBS, pH 7.4.[18] For experimental control, HRECs were grown in normal medium containing PBS.

Mouse Model of Oxygen-Induced Retinopathy and Treatment

Experiments were performed on C57BL/6 mice (Laboratory Animal Center of Zhongshan Ophthalmic Center, Sun Yat-sen University) of both sexes at postnatal day (PD) 17. All experiments were in compliance with the ARVO Statement for the Use of Animals in Ophthalmic and Vision Research, and were approved by the Animal Care Committee of Sun Yat-sen University. The reproducible murine model of oxygen-induced retinopathy (OIR) has been described previously.[19] Briefly, mice pups with their nursing mothers were exposed to room air between PD 1 and PD 17, using as normal controls (Group 1: normal mice). Mice of the same strain and the same age were exposed to 75% ± 2% oxygen between PD 7 and PD 12, and then returned to room air for 5 days (Group 2: OIR mice). OIR mice

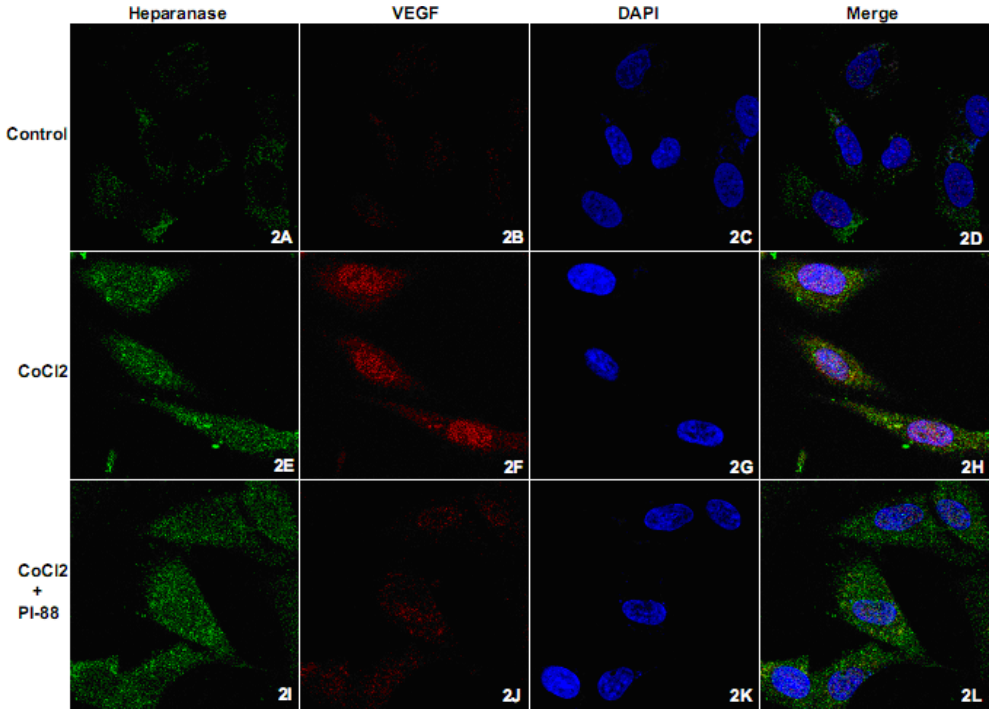

Figure 2. Confocal microscopy analysis of heparanase and VEGF protein levels in $CoCl_2$-treated HRECs. HRECs were cultured in normal media (control; [**A**–**D**]), or treated with $CoCl_2$ (**E**–**H**), or with $CoCl_2$ + PI-88 (**I**–**L**) for 24 hours. Cells were stained with DAPI (*blue*; [**C**, **G**, **K**]), and rabbit anti-heparanase (*green*; [**A**, **E**, **I**]) and mouse anti-VEGF (*red*; [**B**, **F**, **J**]) antibodies. Low levels of heparanase (**A**) and VEGF (**B**) were observed in control HRECs and marked increases in $CoCl_2$-treated cells (**E**, **F**). The intense VEGF staining was decreased (**J**) by PI-88.

were injected intraperitoneally with PI-88 at a dose of 25 mg/kg/day for 5 days from PD 12 to PD 16 (Group 3: OIR mice + PI-88). A vehicle group received sterile PBS alone from PD 12 to PD 16 (Group 4: OIR mice + PBS).[20,21] Animals were anesthetized with intraperitoneal injection of 10% chloral hydrate at a dose of 3 mL/kg (Zhongshan Ophthalmic Center) and then the retinas were isolated after eyes were enucleated.

Enzyme-Linked Immunosorbent Assay (ELISA)

The culture medium of HRECs of each group was centrifuged at 9000 rpm for 30 minutes at 4°C, and the supernatant was collected. The levels of VEGF secreted by HRECs were evaluated using an ELISA kit (R&D Systems, Inc., Minneapolis, MN) according to the manufacturer's instructions. Absorbance at 450 nm was measured by a microplate reader (Bio-Rad, Hercules, CA). The concentration of VEGF in the culture medium was normalized against the number of cells in each culture and expressed as pg/10^5 cells.

Heparanase Activity Assays

HRECs from each group were dissolved in the lysis buffer containing 0.5% triton X-100 and protease inhibitors, and then their activity was assayed using the Heparan Degrading Enzyme Assay Kit (Takara Bio, Inc., Shiga, Japan) according to the manufacturer's instruction. Briefly, samples were diluted in assay buffer and incubated at 37°C for 2 hours under shaking, then incubated in 1 mg/mL streptavidin–peroxidase solution at 37°C for 30 minutes (100 μL /well). Finally, the samples were treated with tetramethylbenzidine for 5 minutes at 37°C. Optical density was read at 450 nm. Results were expressed in mU/μg of cell protein. All washes were performed in PBS containing 0.1% Tween 20.

Immunofluorescence

HRECs were seeded on glass coverslips precoated with 5 mg/mL fibronectin (Gibco) and allowed to grow to semi-confluent in a culture dish. Cells were washed with PBS 3 times and fixed in fresh 4% paraformaldehyde (PFA, pH 7–8) for 10 minutes at room temperature. Next, HRECs were permeabilized in 0.1% Triton X-100 (Sigma) for 5 minutes and blocked with 1% BSA (Sigma) in PBS containing 0.1% Tween 20 (blocking solution) for 60 minutes at room temperature. The cells then were incubated with rabbit anti-human heparanase antibody (1:300 dilution; Abcam, Cambridge, MA) and mouse anti-human VEGF antibody (1:200 dilution; Abcam) overnight at 4°C, followed by incubation with appropriate secondary antibody conjugated with Alexa Fluor 488 and Alexa Fluor 555 (1:200 dilution; Boster Biological Technology, Ltd., Wuhan, China) for 2 hours at room temperature. The cells were stained with 100 ng/mL of 4′,6-diamidino-2-phenylindole (DAPI; Sigma) for 5 minutes, and mounted with an anti-fading fluorescence medium (Vector Laboratories, Burlingame, CA) and then imaged using laser scanning confocal microscope.

Western Blot Analysis

HRECs and the retinas of normal/OIR mice were harvested and lysed in 100 μL lysis buffer containing 150 mM NaCl, 50 mM Tris-HCl (pH 7.5), 0.5% Triton X-100, and protease inhibitors cocktail (Sigma). The cells then were centrifuged at 9000 rpm at 4°C for 30 minutes. The supernatant then was collected and mixed with 2 × sample loading buffer to prepare samples. The total protein from each sample was analyzed by SDS-PAGE using a 10% Tris-glycine gel (Invitrogen, Paisley, UK) and transferred onto a polyvinylidene difluoride membrane (Bio-Rad) at 250 mA for 90 minutes. Each membrane was blocked with 5% skim milk in Tris-buffered saline containing 0.5% Tween 20 for 1 hour at room temperature and incubated with polyclonal rabbit anti-human/mouse heparanase antibody (1:300 dilution; Abcam) or polyclonal mouse anti-human/mouse VEGF antibody (1:500 dilution; Abcam) at 4°C overnight, followed by incubation with horseradish peroxidase-conjugated secondary antibody for 2 hours at room temperature. Membranes were reprobed with β-actin (1:1000 dilution; Sigma) to confirm equal loading. Finally, the blots were developed with a

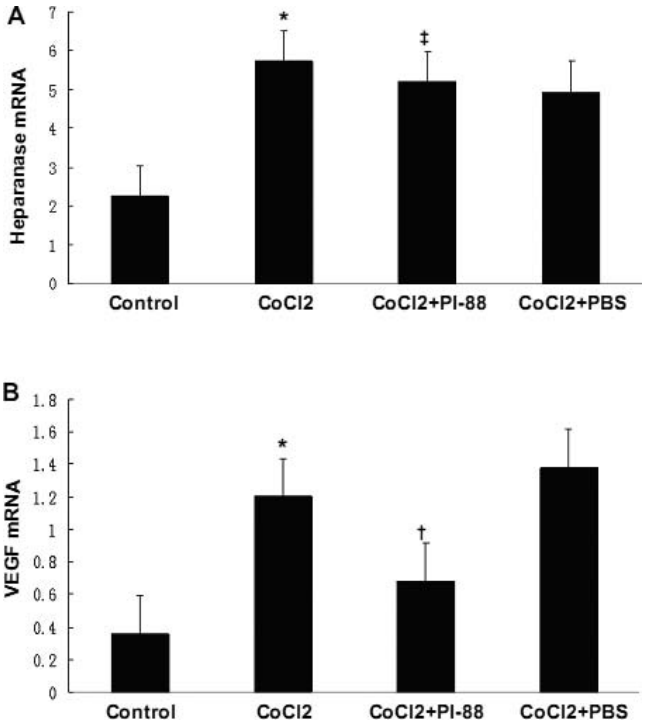

Figure 3. Heparanase and VEGF mRNA levels in $CoCl_2$-treated HRECs. HRECs were cultured with normal medium (control), or treated with $CoCl_2$, $CoCl_2$ + PI-88, and $CoCl_2$ + PBS. The comparative CT method (△△CT) was used for relative quantification. Real-time PCR was performed to detect the mRNA level of heparanase (**A**) and VEGF (**B**). Expression of heparanase (**A**) and VEGF (**B**) was increased in the $CoCl_2$ group compared to that in the controls, and VEGF expression was decreased significantly in the $CoCl_2$ + PI-88 group, but not in the $CoCl_2$ + PBS group. *$P < 0.05$ versus control. †$P < 0.05$ versus $CoCl_2$ or $CoCl_2$ + PBS. ‡$P > 0.05$ versus $CoCl_2$.

chemiluminescence reagent (Cell Signaling Technology Inc, Danvers, MA). Semiquantitative analysis was performed by measuring the optical densities of the bands using Image J (version 1.44p, available online at http://rsbweb.nih.gov/ij). Experiments were repeated 3 times.

Retinal Frozen Section Immunofluorescence

Eyes were enucleated after mice were anesthetized deeply with intraperitoneal injection of 10% chloral hydrate (3 mL/kg). Globes then were embedded in optimal cutting temperature compound (OCT), sectioned at 6 μm, and mounted. The flat mounted sections then were fixed with chilled fresh acetone for 10 minutes, permeabilized in 0.1% Triton X-100 in PBS for 5 minutes, and then blocked with 5% BSA in PBS for 1 hour at room temperature. Retinal sections then were incubated with primary antibodies overnight at 4°C, followed by 1 hour of incubation with secondary antibodies and 5 minutes of incubation with DAPI. Finally, image acquisition was conducted with a laser scanning confocal microscope.

Flat Mounts of High Molecular Weight FITC-Dextran Perfused Retina

Mice were anesthetized deeply by intraperitoneal injection of 10% chloral hydrate (3 mL/kg) and sacrificed by intracardiac perfusion with 1 mL of 50 mg/mL FITC-dextran (molecular weight 2,000,000; Sigma). Then eyes were enucleated and fixed in 4% paraformaldehyde for 1 hour at room temperature. Retinas were dissected and flat mounted on slides with anti-fading fluorescence medium. Images of each of 4

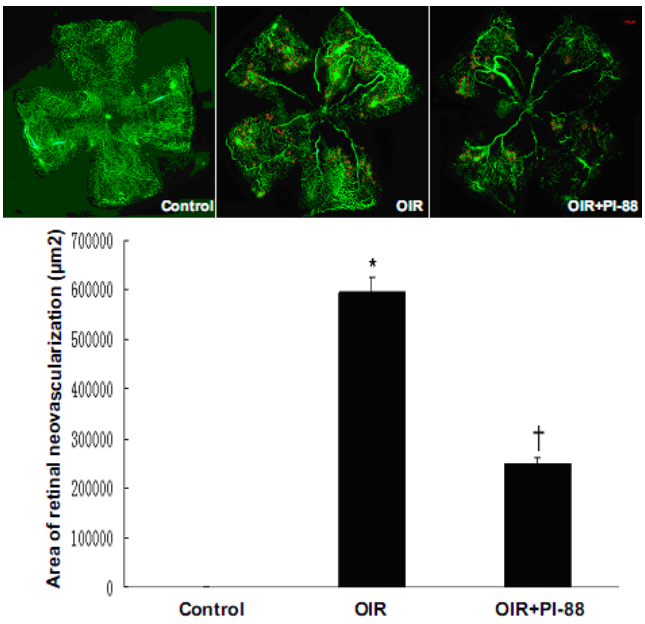

Figure 4. Induction of neovascularization in OIR mice. OIR mice either were untreated (OIR) or injected intraperitoneally with PI-88 at a dose of 25 mg/kg/day for 5 days (OIR + PI-88). Mice then were sacrificed and retinal flat mounts with high molecular weight fluorescein FITC-dextran were performed. Normal mice were used as control. Fluorescence microscopy of representative retinal whole mounts (*upper panel*) was performed to show neovascularization (*red*) and capillary-free areas in retina of OIR mice (PD 17). Original magnification was × 5. The retinal neovascularization areas were quantified (*lower panel*) using Image-Pro Plus (Version 5.1.2.59). We selected the neovascularization region of the retina in the ×5 magnification (*shown in red line circle*), measured the area of the circle according to the magnification matched scale. At least three retinas were selected from each group for measurement and statistical analysis. Data represent the mean ± SD of three independent experiments. *$P < 0.05$ versus control. †$P < 0.05$ versus OIR.

quadrants of the retina were taken at ×5 magnifications on a fluorescence microscope (Axiovert100; Zeiss, Inc., Germany) and imported into Adobe Photoshop software to merge an image of the entire retina. Quantitative analysis was performed by measuring the area of retinal neovascularization using Image-Pro Plus (Version 5.1.2.59). We selected the neovascularization region of the retina in the ×5 magnification (shown in red line circle), measured the area of the circle according to the magnification matched scale. At least three retinas were selected from each group for measurement and statistical analysis.

RNA Extraction and Real-Time PCR Analysis

Total RNA was extracted from HRECs/mice retinas with TRIzol reagent (Takara Bio, Inc.) and subsequently reverse transcribed into cDNA using PrimeScript RT reagent Kit (Takara Bio, Inc.) according to the manufacturer's instructions. Real-time PCR was performed using the SYBR Premix Ex Taq Kit (Takara Bio, Inc.) in a 20 μL reaction volume containing 10 μL SYBR Premix Ex Taq, 0.4 μL each of specific primer, 0.4 μL ROX Reference Dye, 2 μL cDNA, and 6.8 μL RNase free dH_2O. Samples were run in duplicates in 96-well plates (Bio-Rad) with heparanase specific primers (forward, CAAGAACAGCACCTACTCAAG; reverse, AGCAGTAGTCAAGGAGAAGC), VEGF specific primers (forward, ATCTT CAAGCCGTCCTGTGT; reverse, GCATTCACATCTGCTGTGCT), and β-actin primers (forward, TCTACAATGAGCTGCGTGTG; reverse, GCAA CATAGCACAGCTTCTC). The comparative CT method (△△CT) was used for relative quantification.

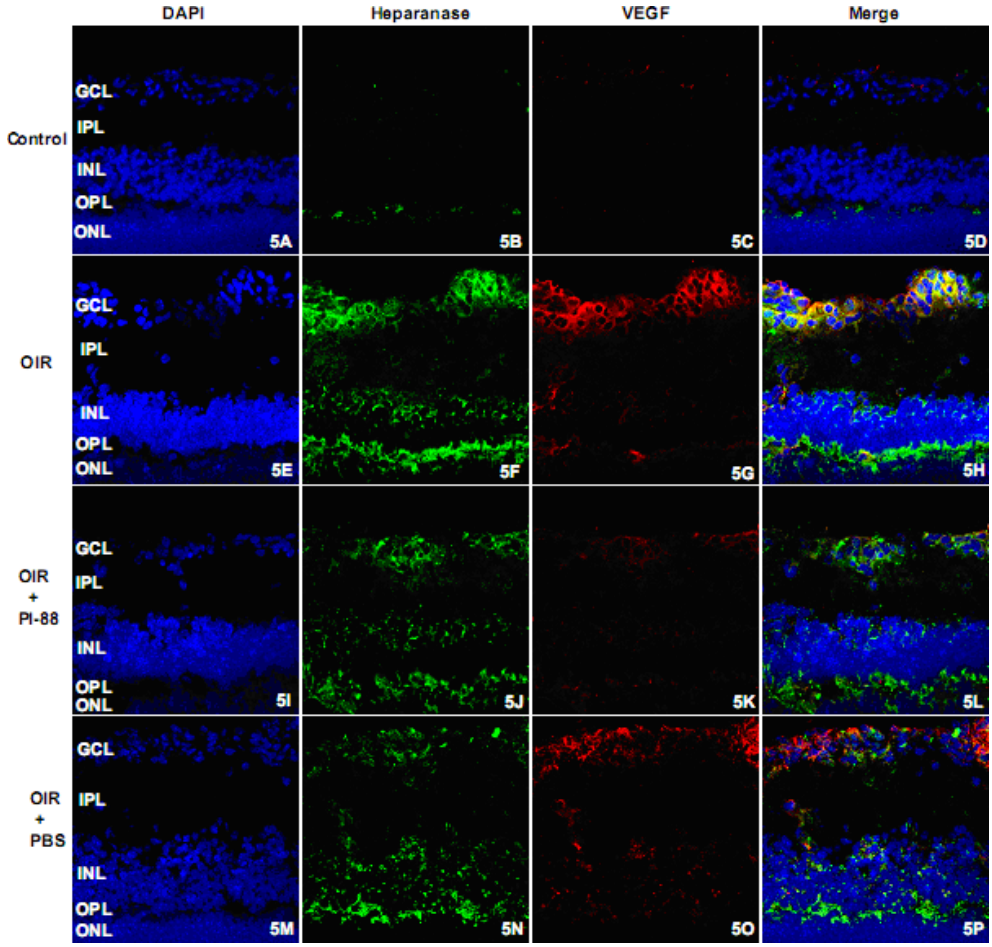

Figure 5. Heparanase and VEGF expression in the retina of OIR mice. OIR mice were left untreated (OIR; [**E**–**H**]), or treated with PI-88 (OIR + PI-88; [**I**–**L**]) or PBS (OIR + PBS; [**M**–**P**]). Mice were sacrificed and eyes were enucleated. Fluorescence confocal microscopy of retinal frozen sections then was performed using DAPI (*blue*; [**A**, **E**, **I**, **M**]) and rabbit anti-heparanase (*green*; [**B**, **F**, **J**, **N**]) or mouse anti-VEGF (*red*; [**C**, **G**, **K**, **O**]) antibodies. Normal mice (**A**–**D**) were used as control. *Magnification*: ×400. GCL, ganglion cell layer; IPL, inner plexiform layer; INL, inner nuclear layer; OPL, outer plexiform layer; ONL, outer nuclear layer.

Statistical Analysis

Data were analyzed and graphs were generated using Prism (version 4.0, GraphPad software). Statistical significance was analyzed by performing one-way ANOVA or Student's *t*-test. P values < 0.05 were considered to be statistically significant.

Results

Effect of the Hypoxia Mimetic Agent $CoCl_2$ on Heparanase Activity and Expression of Heparanase and VEGF in HRECs

To characterize the effect of the hypoxia mimetic agent $CoCl_2$ on HREC heparanase enzymatic activity, HRECs were incubated with 100 μM $CoCl_2$ for 24 hours. Heparanase activity was increased 2.95-fold compared to the control ones (untreated HRECs, $P = 0.019 < 0.05$, Fig. 1A). The increased activity was partially decreased (1.32-fold) in $CoCl_2$-treated cells in the presence of 5 μg/mL PI-88 ($P = 0.036 < 0.05$, Fig. 1A).

To investigate the effect of $CoCl_2$ on the expression of heparanase and VEGF in HRECs, we performed ELISA for VEGF, and immunofluorescence, real-time PCR, and Western blot analysis for heparanase and VEGF. In initial experiments, we confirmed the expression of heparanase and VEGF in HRECs by immunoblot analysis (Figs. 1B, 1C). Immunoblot analysis of HERCs that were untreated (control), or treated with $CoCl_2$ (100 μM) for 24 hours ($CoCl_2$), with $CoCl_2$ and PI-88 (5 μg/mL) for 24 hours ($CoCl_2$ + PI-88), and with $CoCl_2$ and PBS ($CoCl_2$ + PBS), revealed that $CoCl_2$ treatment resulted in a substantial increase in heparanase and VEGF proteins. HRECs heparanase and VEGF protein levels were increased by 1.55-fold and 2.38-fold after $CoCl_2$ treatment for 24 hours compared to the untreated control cells (heparanase 0.90 ± 0.10 vs. 0.58 ± 0.05, $P = 0.003 < 0.05$; VEGF 0.81 ± 0.24 vs. 0.34 ± 0.08, $P = 0.004 < 0.05$). VEGF protein was decreased by 1.80-fold in $CoCl_2$-treated cells with PI-88 present (0.45 ± 0.09 vs. 0.81 ± 0.24, $P = 0.017 < 0.05$), but not in cells treated with the PI-88 vehicle PBS ($P = 0.369 > 0.05$). This result was confirmed by an ELISA analysis, showing that VEGF was increased significantly by 2.54-fold in $CoCl_2$-treated HRECs compared to the untreated control cells (93.10 ± 14.37 pg/10^5 cells vs. 36.59 ± 16.47 pg/10^5 cells, $P = 0.000 < 0.05$, Fig. 1D) This effect was reduced when the HRECs were grown in the presence of PI-88, showing a 1.42-fold decrease in VEGF level (65.23 ± 5.73 pg/10^5 cells vs. 93.10 ± 14.37 pg/10^5 cells, $P = 0.037 < 0.05$, Fig. 1D). Immunofluorescence staining showed positive staining for heparanase and VEGF in the HRECs after treatment with $CoCl_2$ for 24 hours (Fig. 2). Only faint staining for VEGF was detected in $CoCl_2$-treated cells following PI-88 co-treatment. No VEGF staining was observed in control cells. Interestingly,

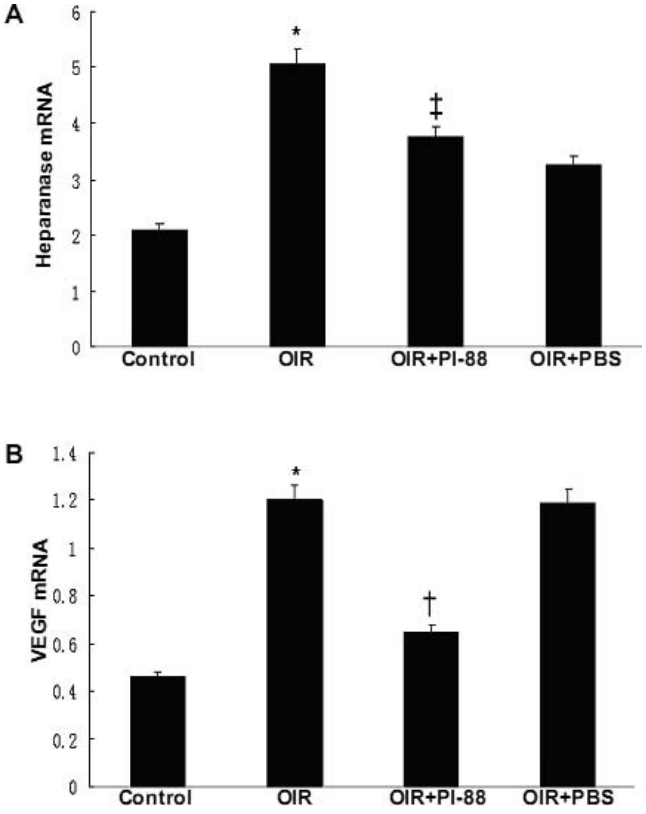

Figure 6. Heparanase and VEGF mRNA levels in the retina of OIR mice. OIR mice were untreated (OIR) or treated with PI-88 (OIR + PI-88) or PBS vehicle (OIR + PBS). Normal mice were used as control. Real-time quantitative PCR was performed to show that expression of heparanase (**A**) and VEGF (**B**) was increased in the OIR mice compared to that in the control ones, and VEGF expression was decreased significantly in the OIR + PI-88 group, but not in the OIR + PBS group. *$P < 0.05$ versus control. †$P < 0.05$ versus OIR or OIR + PBS. ‡$P > 0.05$ versus OIR.

enhanced VEGF staining was found to be localized in the cytoplasm and nucleus. Real-time PCR result (Fig. 3) also showed that, compared to control cells, heparanase mRNA of $CoCl_2$-treated cells was increased (5.73 ± 0.53 vs. 2.25 ± 0.28, $P = 0.003 < 0.05$, Fig. 3A), as well as VEGF mRNA (1.20 ± 0.02 vs. 0.36 ± 0.07, $P = 0.001 < 0.05$, Fig. 3B). Meanwhile, as shown in Figure 3B, VEGF mRNA levels were decreased in cells treated with PI-88 (0.69 ± 0.07 vs. 1.20 ± 0.02, $P = 0.008 < 0.05$, Fig. 3B) but not PBS ($P = 0.264 > 0.05$).

Induction of Neovascularization in OIR Mice Retina

The above study has demonstrated that heparanase is upregulated and associated with VEGF expression in hypoxia-induced HRECs in vitro. To investigate further the neovascularization induced by hypoxia in vivo, we performed retinal flat mounts with high molecular weight FITC-dextran in OIR mice. A large amount of new retinal vessels, which noticeably were absent in control mice, were observed in PD17 OIR mice (549,222.60 ± 212,484.34 μm^2 vs. 0.00 ± 0.00 μm^2, $P = 0.046 < 0.05$). The number of new vessels was decreased by 2.21-fold following intraperitoneal injection of PI-88 at a dose of 25 mg/kg/day for 5 days (248,314.20 ± 129,211.55 μm^2 vs. 549,222.60 ± 212,484.34 μm^2, $P = 0.049 < 0.05$, Fig. 4).

Increased Expression of Heparanase and VEGF in OIR Mouse Retinas

To determine whether heparanase and VEGF expression was increased at the protein level in the retina in vivo, retinal frozen section and immunofluorescence were performed in OIR mice. As shown in Figure 5, staining of heparanase (Fig. 5F) and VEGF (Fig. 5G) in the ganglion cell layer, inner plexiform layer, and outer plexiform layer in OIR mice was more intense than for mice raised under normal conditions. Heparanase and VEGF staining was observed in the ganglion cell layer, where retinal new vessels mainly were distributed and protruded into the vitreous cavity. The VEGF signal was faint (Fig. 5K) when the OIR mice were treated with PI-88 for 5 days, revealing the inhibitory effect of PI-88 on the VEGF expression.

The expression of heparanase and VEGF in the retina of OIR mice was further analyzed quantitatively with real-time PCR. Compared to control retinas, relative hypoxia-induced by 5 days of normoxia after hyperoxia increased the amount of heparanase mRNA by 2.03-fold (4.26 ± 1.36 vs. 2.10 ± 0.14, $P = 0.023 < 0.05$, Fig. 6A) and VEGF mRNA by 2.61-fold (1.20 ± 0.09 vs. 0.46 ± 0.19, $P = 0.004 < 0.05$, Fig. 6B). As shown in Figure 6B, VEGF mRNA levels in OIR mice were decreased by PI-88 (0.64 ± 0.15 vs. 1.20 ± 0.09, $P = 0.004 < 0.05$) but not by PBS ($P = 0.957 > 0.05$). Western blot analysis also showed a similar pattern of increased levels of heparanase and VEGF proteins in the retinas of OIR mice compared to those in normoxia (heparanase 0.97 ± 0.02 vs. 0.64 ± 0.07, $t = 8.139$, $P = 0.007 < 0.05$; VEGF 0.93 ± 0.05 vs. 0.40 ± 0.05, $t = 13.228$, $P = 0.001 < 0.05$, Figs. 7A, 7B). VEGF protein in the retinas of OIR mice was decreased 1.41-fold by PI-88 (0.66 ± 0.05 vs. 0.93 ± 0.05, $t = -6.798$, $P = 0.002 < 0.05$, Fig. 7B).

Discussion

ROP is a leading cause of childhood blindness, and is characterized by retinal hypoxia-ischemia and neovascularization.[1,2] Despite many reports documenting retinal neovascularization, the mechanism involved in angiogenesis in retina remains to be elucidated. Angiogenesis is a complex multifactorial and multi-mechanism process.[22,23] Many causes, including hypoxia, hyperglycemia, and ischemia, can lead to retinal neovascularization.[3,4] VEGF, which has been shown to be upregulated by hypoxia and ischemia, is one of the most significant factors involved in retinal diseases associated with pathologic angiogenesis, including ROP.[3–6] Heparanase, an endo-β-glucuronidase that specifically cleaves HS, is another important molecule that facilitates angiogensis.[11] By degrading HS side chains, heparanase promotes endothelial cell migration and the release of HS-bound angiogenic growth factors, including FGF-2 and VEGF, thereby facilitating angiogenesis in tumors.[24] Meanwhile, the release of HS fragments promotes angiogenic growth factor activity, further enhancing angiogenesis. Here, we provide evidence that heparanase is involved in retinal angiogenesis via an alternative mechanism, in which heparanase regulates VEGF expression in vitro and in vivo under hypoxic and hypoxia mimic conditions.

In our study, we confirmed that heparanase activity was increased in HRECs treated with the hypoxia mimic $CoCl_2$. This suggests that hypoxia could increase the activity of heparanase. Similarly, we have shown in vitro, using Western blot, ELISA, and immunofluorescence approaches, that heparanase and VEGF protein levels were increased in HRECs treated with $CoCl_2$. The increase of VEGF protein level was inhibited when HRECs were treated with heparanase inhibitor PI-88.[25] This suggests that heparanase may be involved in the

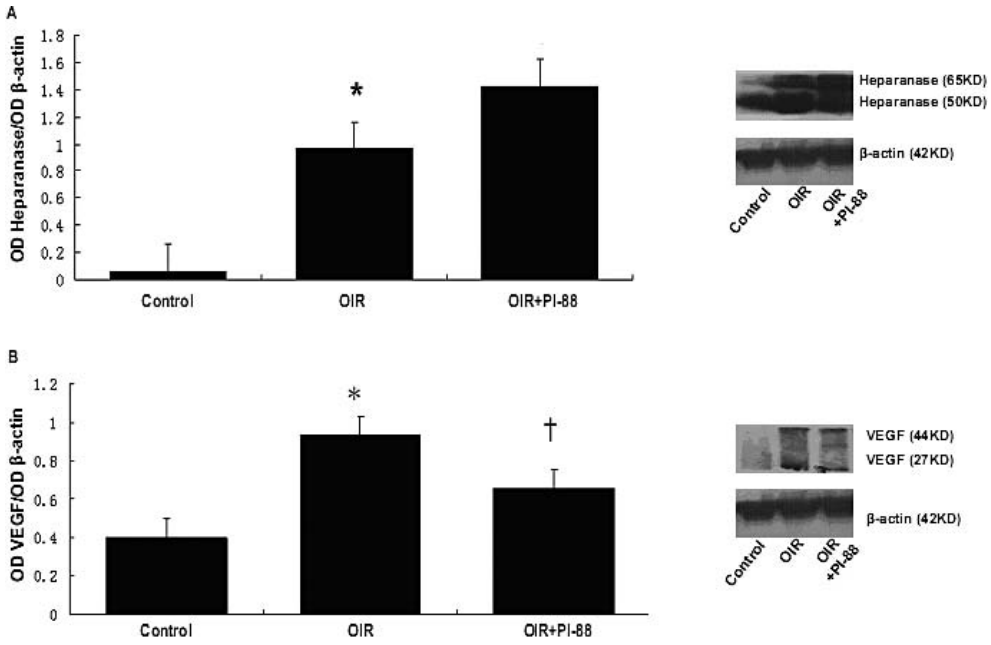

Figure 7. Heparanase and VEGF protein levels in the retina of OIR mice. OIR mice were either untreated (OIR) or treated with PI-88 (OIR + PI-88). Western blot analysis was performed to detect the protein level of heparanase ([**A**], *right panel*) and VEGF ([**B**], *right panel*). Retinas of mice raised under normal condition were used as control (control). The densitometry analysis was performed on the bands using Image J (version 1.44p; [**A**, **B**], *left panel*). Data represent the mean ± SD of three experiments. $^*P < 0.05$ versus control. †$P < 0.05$ versus OIR.

regulation of VEGF expression. Our subsequent in vivo experiments showed that heparanase, VEGF protein, and mRNA levels were increased simultaneously in the retina of OIR mice under hypoxic condition, and this increase was associated with the retinal neovascularization. The increase of VEGF protein and mRNA level was reduced by PI-88, which also was observed in vitro, confirming that heparanase regulates VEGF expression, and is associated with retinal neovascularization under hypoxic and hypoxia mimic conditions in vitro and in vivo. These results are consistent with our previous study, in which it was shown that heparanase and VEGF expression increased at the same time in diabetic retinopathy, which also was characterized by retinal neovascularization.[26] We also have shown that in streptozotocin-induced diabetic rats, PI-88 can inhibit significantly retinal leukostasis, and decrease ICAM-1 and VEGF expression.[27] Together, our studies suggested a regulation role of heparanase upon VEGF in hypoxia-induced retinal diseases.[14,28,29] Previously, it has been shown that overexpression of heparanase in human embryonic kidney 293, MDA-MB-435 human breast cancer, and rat C6 glioma cells results in increased VEGF protein and mRNA levels, and correlates with increased tumor vascularity.[14,15]

It is interesting that VEGF also was located in the nucleus as well as in the cytoplasm of HERCs. The exact function of the nuclear VEGF still is not clear. It has been shown that nuclear localization of VEGF correlated with endothelial cell recovery in wounding in vitro.[30] Other research has suggested that nuclear localization of a long isoform of VEGF that is extended by an additional 180 amino acids, is associated with hypoxia and tumor angiogenesis.[31] Our findings are consistent with these previous studies. A recent study suggested that VEGFR2, the major mediator of the angiogenic effects of VEGF, translocated into the nucleus to regulate its own transcription.[32] The finding that VEGF mRNA, and the increase of VEGF protein in the nucleus of HRECs and the retina of OIR mice upon hypoxia indicates that VEGF also may act as a regulation element of transcription, which deserves to be investigated further.

In conclusion, we provided evidence that heparanase and VEGF are involved in retinal angiogenesis under hypoxic and hypoxia mimic conditions in vitro and in vivo. We showed that heparanase and VEGF are upregulated in hypoxia-induced retinal neovascularization, and inhibition of heparanase results in down-regulation of VEGF expression and less new vessels, suggesting a regulation role of heparanase on the VEGF expression. Heparanase may be a possible new therapeutic target for retinal diseases that are characterized with retinal hypoxia-ischemia, such as ROP.

References

1. Chen J, Smith LE. Retinopathy of prematurity. *Angiogenesis*. 2007;10:133–140.
2. Foos RY. Retinopathy of prematurity. Pathologic correlation of clinical stages. *Retina*. 1987;7:260–276.
3. Ferrara N, Gerber HP, Lecouter J. The biology of VEGF and its receptors. *Nat Med*. 2003;9:669–676.
4. Aiello LP, Northrup JM, Keyt BA, Takagi H, Iwamoto MA. Hypoxic regulation of vascular endothelial growth factor in retinal cells. *Arch Ophthalmol*. 1995;113:1538–1544.
5. Robinson GS, Aiello LP. Angiogenic factors in diabetic ocular disease: mechanisms of today, therapies for tomorrow. *Int Ophthalmol Clin*. 1998;38:89–102.
6. Adamis AP, Miller JW, Bernal MT, et al. Increased vascular endothelial growth factor levels in the vitreous of eyes with proliferative diabetic retinopathy. *Am J Ophthalmol*. 1994; 118:445–450.
7. Mintz-Hittner HA, Best LM. Antivascular endothelial growth factor for retinopathy of prematurity. *Curr Opin Pediatr*. 2009; 21:182–187.
8. Darlow BA, Gilbert C, Quinn GE. Promise and potential pitfalls of anti-VEGF drugs in retinopathy of prematurity. *Br J Ophthalmol*. 2009;93:986.

9. Nicholson BP, Schachat AP. A review of clinical trials of anti-VEGF agents for diabetic retinopathy. *Graefes Arch Clin Exp Ophthalmol*. 2010;248:915–930.
10. Vreys V, David G. Mammalian heparanase: what is the message? *J Cell Mol Med*. 2007;11:427–452.
11. Bame KJ. Heparanases: endoglycosidases that degrade heparan sulfate proteoglycans. *Glycobiology*. 2001;11:91R–98R.
12. Brown J. The hypoxic cell: a target for selective cancer therapy—eighteenth Bruce F. Cain Memorial Award lecture. *Cancer Res*. 1999;59:5863–5870.
13. He X, Brenchley PE, Jayson GC, Hampson L, Davies J, Hampson IN. Hypoxia increases heparanase-dependent tumor cell invasion, which can be inhibited by antiheparanase antibodies. *Cancer Res*. 2004;64:3928–3933.
14. Zetser A, Bashenko Y, Edovitsky E, et al. Heparanase induces vascular endothelial growth factor expression: correlation with p38 phosphorylation levels and Src activation. *Cancer Res*. 2006;66:1455–1463.
15. Vlodavsky I, Ilan N, Naggi A, Casu B. Heparanase: structure, biological functions, and inhibition by heparin-derived mimetics of heparan sulfate. *Curr Pharm Res*. 2007;13:2057–2073.
16. Li B, Tang SB, Hu J, et al. Protective effects of transcription factor HESR1 on retinal vasculature. *Microvasc Res*. 2006;72:146–152.
17. Ryan HE, Poloni M, McNulty W, et al. Hypoxia-inducible factor-1α is a positive factor in solid tumor growth. *Cancer Res*. 2000;60:4010–4015.
18. Parish CR, Freeman C, Brown KJ, Francis DJ, Cowden WB. Identification of sulfated oligosaccharide-based inhibitors of tumor growth and metastasis using novel in vitro assays for angiogenesis and heparanase activity. *Cancer Res*. 1999;59:3433–3441.
19. Smith LE, Wesolowski E, McLellan A, et al. Oxygen-induced retinopathy in the mouse. *Invest Ophthalmol Vis Sci*. 1994;35:101–111.
20. Levidiotis V, Freeman C, Punler M, et al. A synthetic heparanase inhibitor reduces proteinuria in passive Heymann nephritis. *J Am Soc Nephrol*. 2004;15:2882–2892.
21. Parish CR, Freeman C, Brown KJ, Francis DJ, Cowden WB. Identification of sulfated oligosaccharide-based inhibitors of tumor growth and metastasis using novel in vitro assays for angiogenesis and heparanase activity. *Cancer Res*. 1999;59:3433–3441.
22. Kubota Y, Suda T. Feedback mechanism between blood vessels and astrocytes in retinal vascular development. *Trends Cardiovasc Med*. 2009;19:38–43.
23. Vlodavsky I, Korner G, Ishai-Michaeli R, Bashkin P, Bar-Shavit R, Fuks Z. Extracellular matrix-resident growth factors and enzymes: possible involvement in tumor metastasis and angiogenesis. *Cancer Metastasis Rev*. 1990;9:203–226.
24. Vlodavsky I, Elkin M, Pappo O, et al. Mammalian heparanase as mediator of tumor metastasis and angiogenesis. *Isr Med Assoc J*. 2000;2(suppl):37–45.
25. Kudchadkar R, Gonzalez R, Lewis KD. PI-88: a novel inhibitor of angiogenesis. *Expert Opin Investig Drugs*. 2008;17:1769–1776.
26. Ma PP, Luo Y, Hu J, et al. Retinal heparanase expression in streptozotocin-induced diabetic rats. *Can J Ophthalmol*. 2010;45:46–51.
27. Ma PP, Luo Y, Hu J, et al. Phosphomannopentaose sulfate (PI-88) inhibits retinal leukostasis in diabetic rat. *Biochem Biophys Res Commun*. 2009;380:402–406.
28. Rivera RS, Nagatsuka H, Siar CH, et al. Heparanase and vascular endothelial growth factor expression in the progression of oral mucosal melanoma. *Oncol Rep*. 2008;19:657–661.
29. Naomoto Y, Gunduz M, Takaoka M, et al. Heparanase promotes angiogenesis through Cox-2 and HIF1alpha. *Med Hypotheses*. 2007;68:162–165.
30. Santos SC, Miguel C, Domingues I, et al. VEGF and VEGFR-2 (KDR) internalization is required for endothelial recovery during wound healing. *Exp Cell Res*. 2007;313:1561–1574.
31. Rosenbaum-Dekel Y, Fuchs A, Yakirevich E, et al. Nuclear localization of long-VEGF is associated with hypoxia and tumor angiogenesis. *Biochem Biophys Res Commun*. 2005;332:271–278.
32. Domingues I, Rino J, Demmers JA, de Lanerolle P, Santos SC. VEGFR2 translocates to the nucleus to regulate its own transcription. *PLoS One*. 2011;6:e25668.